PR2 Advancement of integrated system for dose estimation in BNCT

Y. Sakurai

Institute for Integrated Radiation and Nuclear Science, Kyoto University

BACKGROUNDS AND PURPOSES:

Several types of accelerator-based irradiation system for boron neutron capture therapy (BNCT) are under development at present. But, there are a number of subjects, which should be improved for the further advance and generalization of BNCT.

In the viewpoints of medical physics and engineering, the advance for dose estimation is one of the important subjects. For the characterization of irradiation field, quality assurance and quality control (QA/QC), clinical irradiation to actual patient, and so on, an ultimate goal is to perform the three-dimensional and real-time dose estimation in discriminating for thermal, epi-thermal and fast neutron doses, gamma-ray dose, and boron dose, with simplicity and low effort. Considering about this ultimate dose estimation, several kinds of dose estimation method are studied. It is so difficult to realize the ultimate dose estimation using only one method, but it is necessary to use simultaneously more than two methods.

The purposes of this project research are the advance for various dose estimation methods, and the establishment of an integrated system for dose estimation in BNCT.

In the third year of this research project, 2022, the advancement for the respective dose estimation methods were forwarded mainly using Heavy Water Neutron Irradiation Facility (HWNIF) and E-3 Neutron Guide Tube (E-3) at KUR, sequentially the previous year. In addition, the integrated system was considered for the simultaneous usage of several dose estimation methods

RESEARCH SUBJECTS:

The collaboration and allotted research subjects (ARS) were organized as follows;

ARS-1 (R4P2-1): Establishment of characterization estimation method in BNCT irradiation field using Bonner sphere and ionization chamber (VI). (Y. Sakurai, A. Sasaki, N. Matsubayashi, M. Nojiri, D. Fu, T. Takata, H. Tanaka)

ARS-2 (R4P2-2): Study on neutron energy spectrometry for epi-thermal neutrons. (S. Yoshihashi, A. Yamazaki, K. Watanabe, Y. Oshima, A. Uritani, Y. Sakurai)

ARS-3 (R4P2-3): Development of Bonner sphere spectrometer using small lithium-glass scintillator for intense neutron beams. (A. Masuda, T. Matsumoto, S. Manabe, K. Watanabe, A. Ishikawa, H. Tanaka, Y. Sakurai, H. Harano, T. Takata, A. Uritani)

ARS-4 (R4P2-4): Improvement of the SOF detector system for energy-dependent discrimination and long-term stability. (M. Ishikawa, S. Ishiguri, K. Takamiya, Y. Sakurai)

ARS-5 (R4P2-5): Improvement of absolute fast neutron flux intensity monitor for BNCT. (I. Murata, K. Sagara, R. Kawahata, S. Tamaki, S. Kusaka, H. Tanaka, Y. Sakurai, T. Takada)

ARS-7 (R4P2-7): Neutron image sensor for boron neutron capture therapy. (M. Taniguchi, T. Meguro, H. Tanaka, S.-I. Kuroki)

ARS-8 (R4P2-8): Preliminary survey of nuclide for epithermal neutron measurement using gel detector. (K. Tanaka, Y. Sakurai, T. Kajimoto, H. Tanaka, T. Takata, S. Endo)

ARS-9 (R4P2-9): Measurements of neutron fluence and gamma ray distribution using thermoluminescence slabs. (K. Shinsho, N. Sugioka, E. Sasaki, H. Tanaka, T. Takata, W. Chang, S. Matsumoto, G. Wakabayashi, G. Okada, Y. Koba)

ARS-11 (R4P2-11): Development and evaluation of 3D gel dosimeter for the measurement of dose distribution in BNCT. (S. Hayashi, Y. Sakurai, M. Suzuki, T. Takata)

ARS-12 (R4P2-12): Establishment of beam-quality estimation method in BNCT irradiation field using dual phantom technique (VI). (Y. Sakurai, N. Kondo, T. Takata, H. Tanaka, M. Suzuki)

ARS-13 (R4P2-13): Development of real-time boron-concentration estimation method using gamma-ray telescope system for BNCT. (Y. Sakurai, D. Fu, T. Takata, H. Tanaka, M. Suzuki)

ARS-14 (R4P2-14): Development of scintillator for thermal neutron detector in BNCT. (N. Matsubayashi, H. Tanaka, S. Kurosawa, A. Yamaji, T. Hanada, T. Takata)

ARS-15 (R4P2-15): Quantitative measurement of 478 keV prompt gamma-rays of boron-neutron capture reaction. (S. Komura, T. Mizumoto, Y. Sakurai, T. Takata, T. Tanimori, H. Kimura, A. Takada)

ARS-16 (R4P2-16): Visualization of boron dose distribution on a borosilicate glass plate by neutron irradiation. (A. Nohtomi, Y. Kojima, H. Maeda, T. Yamane, G. Wakabayashi, Y. Sakurai, T. Takata)

ARS-18 (R4P2-18): Investigation of thermal neutron-induced soft errors in semiconductor devices. (H. Tanaka, R. Nakamura, T. Kato)

ARS-19 (R4P2-19): Dosimetric characteristics of optimized bolus for boron neutron capture therapy. (T. Takata, M. Nojiri, A. Sasaki, Y. Sakurai, H. Tanaka, M. Suzuki)

ARS-23 (R4P2-23): Three dimensional humanized oral cancer in vitro model for BNCT. (K. Igawa, K. Izumi, E. Naito, M. Suzuki, N. Kondo, Y. Sakurai)

ARS-24 (R4P2-24): Boron-10 uptake distribution in 3D oral cancer model using CR-39 solid state nuclear track detector. (K. Igawa, R. Ogawara, T. Kusumoto, Y. Sakurai)

ARS-6, ARS-10, ARS-17, ARS-20, ARS-21 and ARS-22 could not be performed mainly because of the influence of COVID-19 infection.

PR2-1 Establishment of characterization estimation method in BNCT irradiation field using Bonner sphere and ionization chamber (VI)

Y. Sakurai, A. Sasaki[1], N. Matsubayashi[1], M. Nojiri[1], D. Fu[1], T. Takata and H. Tanaka

Institute for Integrated Radiation and Nuclear Science, Kyoto University
[1]Graduate School of Engineering, Kyoto University

INTRODUCTION: Development in accelerator-based irradiation systems for BNCT is underway. In the near future, BNCT using these newly developed systems may be carried out at multiple facilities across the world. Considering this situation, it is important that the estimations for dose quantity and quality are performed consistently among several irradiation fields, and that the equivalency of BNCT is guaranteed, within and across BNCT systems. Then, we are establishing QA/QC system for BNCT.

As part of the QA/QC system, we are developing estimation method for neutron energy spectrum using Bonner sphere [1]. For our spectrometer using Bonner sphere, liquid such as pure water and/or boric acid solution is used as the moderator. A multi-layer concentric-sphere case with several sphere shells is prepared. The moderator and its diameter are changeable without entering the irradiation room, by the remote supply and drainage of liquid moderator in the several layers. For the detector, activation foils are remotely changed, or online measurement is performed using SOF detector, etc.

In 2022, verification experiments for the prototype Remote-changeable Bonner-sphere Spectrometer (RBS) were performed using Heavy Water Neutron Irradiation Facility installed in Kyoto University Reactor (KUR-HWNIF) as in the previous year [2].

MATERIALS AND METHODS: In the neutron energy spectrometry by Bonner-sphere, the combinations of the moderator material and diameter should be previously decided and prepared. Of course, the more information can be obtained as the more moderators and detectors are prepared. However, the information number from those measured data is less than the combination number, because of the overlapped regions among the combinations. The selection is important, in which the more information number is obtained for the combination number.

The combination of moderator and detector is decided, for that the response functions cannot be approximated by the linear functions of the other response functions. The accuracy and precision for the spectrometry can be higher, because the independent information can be obtained from the measurement by the respective combinations. We were developed the selection method, High Independence Selection (HIS) [3].

On the assumption of the application in the standard epi-thermal neutron irradiation mode of KUR-HWNIF, the combination of the moderators for boron-10 concentration and diameter was optimized by HIS. Based on this optimization, the prototype RBS was revised. Some experiments were performed for the characteristic verification of the revised prototype RBS at KUR-HWNIF.

RESULTS: The configuration of the revised RBS was decided as follows. A five-layer concentric spherical acrylic shell is used as a container. Each acrylic wall is 1 mm in thickness. The moderator injection part is 9 mm in thickness for each layer. Pure water and 0.12-wt% boric acid water for boron-10 were used as liquid moderators. A LiCaF scintillation detector was used as the detector. Figure 1 shows the outline of the revised prototype RBS.

Unfolding was performed by GRAVEL using the response function of each Bonner sphere corrected by multiplying the ratio for measured/calculated values. The nominal spectrum of the epi-thermal neutron irradiation mode was input as an initial guess.

The comparison between the nominal spectrum and unfolded spectrum was performed. The spectrum obtained by the unfolding reproduced the nominal spectrum relatively and absolutely well. It was confirmed that the accuracy of the revised prototype RBS was more improved than the previous version.

CONCLUSION: We have the plans to perform (1) the further revision of the prototype RBS and (2) the preparation of a Bonner sphere spectrometer including the remote mechanism for the supply and drainage of the liquid moderators.

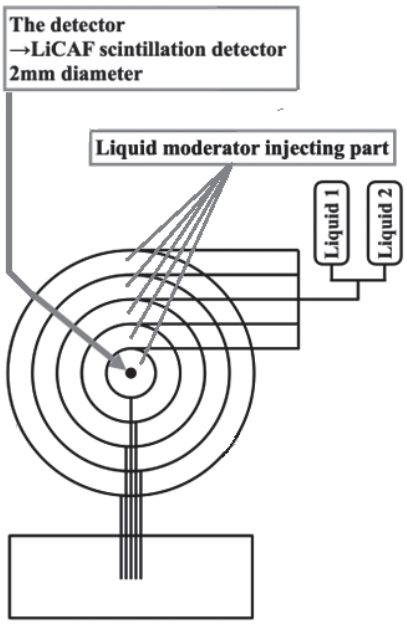

Fig. 1. Outline of the revised prototype of RBS.

REFERENCES:

[1] S. Shiraishi *et al.,* Appl. Radiat. Isot., **163** (2020) 109213.
[2] Y. Sakurai and T. Kobayashi, Nucl. Instr. Meth. A, **453** (2000) 569-596.
[3] H. Ueda, Doctoral Thesis, Kyoto Univ., (2016).

PR2-2 Study on neutron energy spectrometry for epi-thermal neutrons

S. Yoshihashi, A. Yamazaki, K. Watababe[1], Y. Oshima[1], A. Uritani and Y. Sakurai[2]
Graduate School of Engineering, Nagoya University
[1]Graduate School of Engineering, Kyushu University
[2] Institute for Integrated Radiation and Nuclear Science, Kyoto University

INTRODUCTION: Boron neutron capture therapy (BNCT) is one of the radiotherapies. This is a combined modality of radiotherapy and chemotherapy for cancer treatment. In the BNCT, a boron-containing agent, which is concentrated into tumor cells, are irradiated with thermal neutrons and $^{10}B(n,\alpha)$ reactions are induced. The BNCT is radiotherapy using neutrons. Recently, an accelerator-driven neutron source has actively been developed instead of nuclear reactors, owing to its simplicity of management. The energy spectrum of neutrons, which is irradiated to patients, should be evaluated in order to assure safety of patients.

The conventional technique for neutron spectrometry is the Bonner sphere method. The similar concept is the liquid moderator type neutron spectrometer, in which a small neutron detector can be moved and various neutron responses can be acquired. In this study, we are developing a new neutron detector using an optical fiber. So far, in order to realize the optical fiber type neutron detector showing a neutron peak in the pulse height spectrum, bright neutron scintillators, such as Eu:$LiCaAlF_6$ or LiF/Eu:CaF_2 eutectics, have been used [1]. Recently, we attempted to replace them with the faster Li glass scintillator[2]. For the both cases, we have never controlled a shape of scintillators because the scintillator size have been too small. Since they had random shapes, the Monte-Carlo simulation based study was difficult to be conducted. In order to evaluate the accurate detector response, the scintillator shape is required to be controlled.

We proposed that a transparent composite Li glass scintillator, in which fine Li glass scintillator powder and resin are mixed. This type of scintillator is expected to be easily shaped because it is a resin-based material. In this study, we fabricate the optical fiber type neutron detector using the transparent composite Li glass scintillator and evaluate its response to thermal neutron irradiation.

EXPERIMENTS: We fabricated the optical fiber type neutron detector using the transparent composite Li glass scintillator. First, fine powder of the Li glass and UV curable resin were mixed. The mixed resin was attached on a tip of an optical fiber. The resin was spontaneously shaped to a hemispherical shape by surface tension. And then, the mixed resin was irradiated with UV light to solidify it. Figure 1 shows a photograph of the fabricated the optical fiber type detector using the transparent composite Li glass scintillator. The detector was irradiated with thermal neutron beam at E-3 beam port of Kyoto University Reactor.

RESULTS: Figure 2 shows the signal pulse height spectra obtained when the fabricated optical fiber type neutron detector was irradiated with thermal neutron beam at E-3 beam port. The fabricated optical fiber type neutron detector shows a clear neutron peak in the signal pulse height spectrum. The detector can be expected to be used for the neutron energy spectrometer.

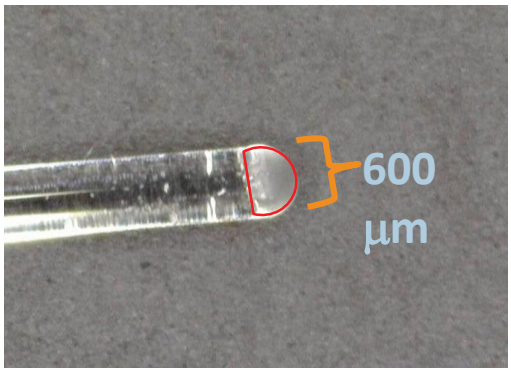

Fig. 1. Photograph of the fabricated optical fiber type neutron detector using the transparent composite Li glass scintillator.

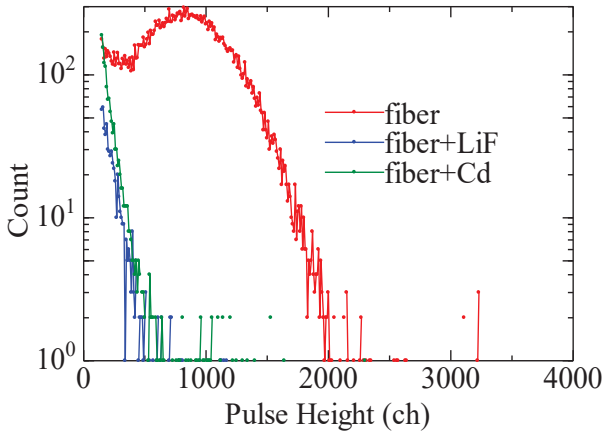

Fig. 2. Signal pulse height spectra obtained from the fabricated optical fiber type neutron detector.

REFERENCES:

[1] K. Watanabe *et al.*, Nucl. Instrum. Methods. Phys. Res. A , **802** (2015) 1-4.
[2] A. Ishikawa *et al.*, Sensors and Materials, **32** (2020) 1489-1495.

PR2-3 Development of Bonner Sphere Spectrometer using Small Lithium-Glass Scintillator for Intense Neutron Beams

A. Masuda, T. Matsumoto, S. Manabe, K. Watanabe[1], A. Ishikawa[2], H. Tanaka[3], Y. Sakurai[3], H. Harano, T. Takata[3] and A. Uritani[2]

National Metrology Institute of Japan, National Institute of Advanced Industrial Science and Technology
[1]Graduate School of Engineering, Kyushu University
[2]Graduate School of Engineering, Nagoya University
[3]Institute for Integrated Radiation and Nuclear Science, Kyoto University

INTRODUCTION: Neutron spectral fluence of intense neutron beams for boron neutron capture therapy (BNCT) should be measured to ensure therapeutic efficacy and safety. Bonner unfolding method is the best known and proven method for measuring neutron spectral fluence [1]. In this study, a small lithium-glass scintillator is adopted to Bonner sphere detectors to suppress the sensitivity of these detectors to accommodate the therapeutic-level neutron intensity.

EXPERIMENTS: A small lithium-glass scintillator coupled with an optical fiber [2] and a photomultiplier tube (PMT, Hamamatsu R9880U-21) was placed at the center of the high-density polyethylene moderator sphere using gapless HDPE fillers, to configure the Bonner sphere detector. Electrical outputs of PMT were processed by a preamplifier (Ortec 113) and a signal processing and acquisition system (Amptek PX5). Diameter of the moderators of the Bonner sphere detectors were 3”, 3.5”, 4”, 4.5”, 5”, 6”, 7” and 8”.
Bonner sphere detectors were placed at a fixed position and irradiated by the standard mixed neutron in the heavy water irradiation facility of the KUR [3], as shown in Fig.1.

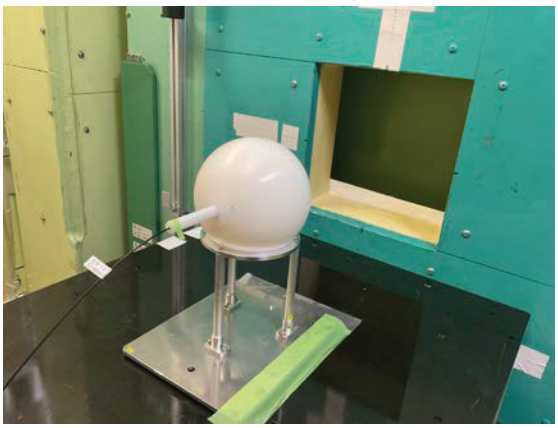

Fig. 1. A Bonner sphere detector equipped with a small lithium-glass placed at the measurement position of the heavy water irradiation facility of the KUR.

RESULTS: Fig. 2 shows output pulse-height spectra from the Bonner sphere detectors with the small lithium -glass scintillator. Pulse signals were properly analyzed and collected by the system, and neutron-induced signals can be discriminated from the photon-induced signals based on the pulse height. Signals above 225 ch were regarded as the neutron induced signals. The background signals which were acquired while neutron beam is off, were negligible. The difference in detection efficiency depending on the sphere diameter was also reasonable. These results show that the developed Bonner sphere detector performed appropriate measurements for intense neutrons.

However, parameters of the signal processing system have not yet been optimized. The effect of the optimization on measurement accuracy is significant, especially in high counting rate measurements. In the future, after optimizing the parameters of the signal processing, spectrum evaluation will be performed by the unfolding method.

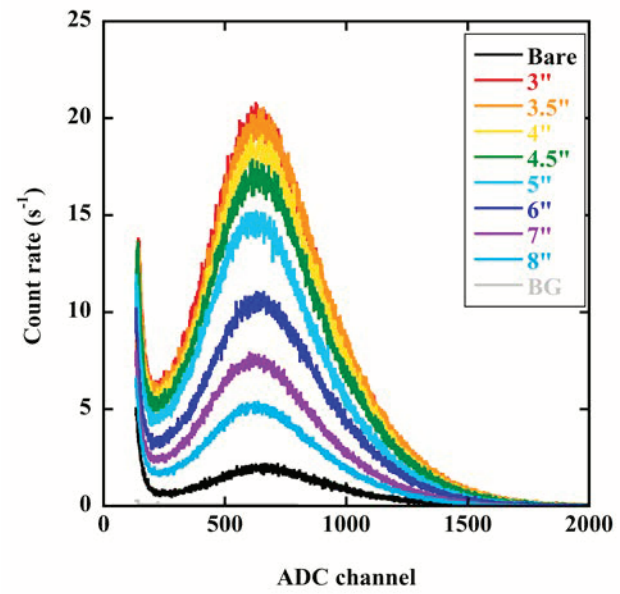

Fig. 2. Pulse-height spectra of the Bonner sphere detector acquired by the signal processing and acquisition system.

REFERENCES:

[1] A. Masuda *et al.,* Appl. Radiat. Isot., **127** (2017) 47-51.
[2] A. Ishikawa *et al.,* Sensors and Materials, **32** (2020) 1489-1495.
[3] Y. Sakurai and T. Kobayashi, Nucl. Instrum. Methods Phys. Res. A, **453** (2000) 569-596.

This study is supported by Grant-in-Aid for Scientific Research, Japan Society for the Promotion of Science (JSPS KAKENHI Grant Number JP22K12667).

PR2-4 Improvement of the SOF detector system for energy-dependent discrimination and long-term stability

M. Ishikawa[1,2], Shu Ishiguri[2], K. Takamiya[3] and Y. Sakurai[3]

[1]*Faculty of Health Sciences, Hokkaido University*
[2]*Graduate School of Biomedical Science and Engineering, Hokkaido University*
[3]*Institute for Integrated Radiation and Nuclear Science, Kyoto University*

INTRODUCTION: We have been conducting research on SOF detectors as thermal neutron flux monitors in BNCT for many years. [1,2] However, degradation of the SOF detector due to long-term irradiation has been reported.[3] As anti-degradation methods, we have replaced plastic optical fibers, which cause degradation, with quartz fibers, and developed degradation monitors using UV photons. In addition, since epithermal neutron irradiation has become mainstream in recent years, it is desirable to be able to measure the epithermal neutron flux.

EXPERIMENTS: In last year's experiment, the measurement was performed with thermal neutron flux of 1×10^{11}[n/cm^2/s] (~30 cm above from the bottom of the slant hole), but this year, measurement was performed with 1×10^{12}[n/cm^2/s] (bottom of the slant hole), one order of magnitude higher neutron intensity. Figure 1 shows the deterioration monitoring system using pulsed UV-LED. In addition to the 1-second interval measurement by the SOF detector, the scintillation light excited by the UV-LED was measured once every 10 seconds to assess the deterioration of the SOF probe. Figure 2 shows the signal count rate of the SOF detector during irradiation. From the Fig. 2, the SOF detector signal attenuated by about 84% during 5 hours of irradiation. The signal attenuation was well represented by a two-component exponential function. The signal from the UV-LED for monitoring showed a constant value and degradation could not be monitored. This is assumed to be because impurities and other contaminants adhered to the connector surface and the excited photons by the UV light were detected as a signal. As a future improvement, visible light which can induce scintillator emission, should be used instead of ultraviolet light.
On the other hand, we tried to establish energy-dependent SOF detector by using different neutron sensitizers, but no effective signal could be obtained. Instead of using different sensitizers, we tried estimating neutron energy spectrum from the measured thermal neutron flux distribution. Figure 3 shows the experimental geometry, a linear actuator was set on a 20 x 20 x 20 cm^3 PMMA phantom filled with water, and thermal neutron flux measurements were performed with SOF detectors at 5 mm-interval in the range of 0.5 to 14.5 cm from the phantom surface. Figure 4 shows that the energy spectrum estimated by unfolding using MLEM. From Fig. 4, good agreement was observed for neutron energies above 1 eV, but a rather large discrepancy in the thermal neutron region. For future work, we would like to improve the MLEM algorithm to increase accuracy in the thermal neutron region.

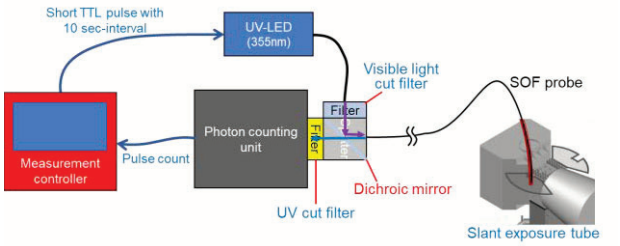

Fig. 1. Schematic illustration of deterioration monitor using pulsed UV-LED.

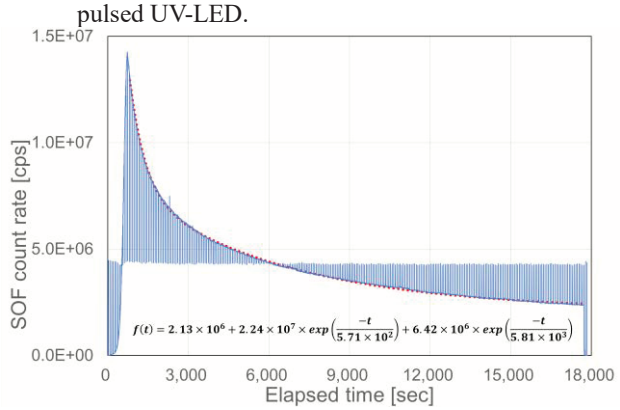

Fig. 2. SOF detector measurement with UV-LED signals.

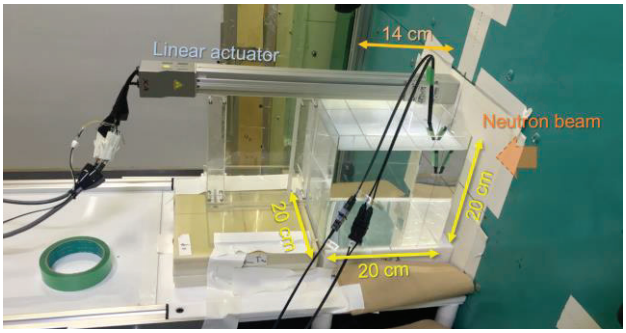

Fig. 3. Measurement geometry for neutron energy spectrum estimation using MLEM unfolding method.

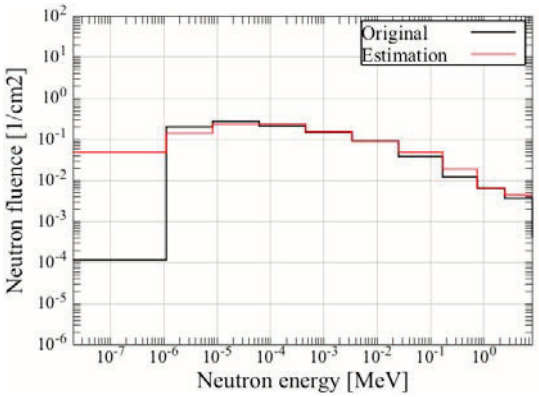

Fig. 4. Estimated neutron energy spectrum by SOF detector.

REFERENCES:

[1] M. Ishikawa *et al.*, Appl. Radiat. Isot., **61** (2004) 775-779.
[2] M. Ishikawa *et al.*, Nucl. Instr. Meth. A, **551** (2005) 448-457.
[3] M. Komeda *et al.*, Appl. Radiat. Isot., **67** (2009) 254-257.

PR2-5 Improvement of Absolute Fast Neutron Flux Intensity Monitor for BNCT

I. Murata, K. Sagara, R. Kawahata, S. Tamaki, S. Kusaka, H. Tanaka[1], Y. Sakurai[1], T. Takada[1]

Graduate School of Engineering, Osaka University
[1]Institute for Integrated Radiation and Nuclear Science, Kyoto University

INTRODUCTION: BNCT is a promising cancer therapy which kills tumor cells while suppressing exposure dose to normal tissues. Normally, the neutron field of BNCT has an energy distribution spreading within thermal and fast regions in addition to epi-thermal region. Because fast neutrons are harmful to the human body, we must measure the fast neutron flux intensity to evaluate the exposure dose of the patient accurately. However, it is quite difficult to know the intensity directly and accurately because there is no suitable neutron spectrometer or no activation material covering epi-thermal or fast neutrons separately. We are therefore developing new monitors to precisely measure the absolute integral flux intensities of fast neutrons (10 keV ~ 1 MeV). [1] In the previous research using the developed detectors to measure the fast neutron flux intensity, the experimental value was underestimated by about 87 % compared to the calculated value. [2] This is because the sensitivity of the previous monitor below 10 keV is not perfectly zero, and the epi-thermal neutron contribution in the neutron spectrum in KUR, Kyoto University, is so large. Therefore, the objective of this study is to modify the monitor to improve its sensitivity and validate it experimentally.

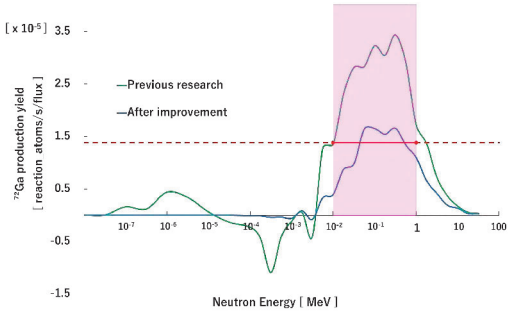

Fig. 1. Comparison of sensitivity between previous monitor and modified monitor.

EXPERIMENTS: According to the previous study, to extract the fast neutron flux intensity, two detectors are used. One of them has a small block-like B_4C in a cubic PE and a GaN foil covered with a Cd sheet at the center of the cubic PE (B_4C type). The other one consists of a cubic PE surrounded by a B_4C sheet and a GaN foil covered with a Cd sheet placed at the center of the cubic PE (PE type). In addition to the above, we designed the detectors by using a ^{10}B neutron shield to suppress the monitor's sensitivity below 10 keV. The modified monitor can estimate the absolute fast neutron flux intensity by making difference of the two ^{72}Ga activities created via $^{71}Ga(n, \gamma)^{72}Ga$ reaction. Fig. 1 shows the comparison of sensitivities between the previous monitor and modified monitor. In this study, the performance of the fast neutron monitor was verified experimentally at KUR. Epi-thermal neutron irradiations were carried out for 50 min in 1 MW operation for each detector.

RESULTS: From Fig. 1, the monitor's sensitivity below 10keV is successfully improved (suppressed to be ~0) by the revision using a ^{10}B neutron shield. The improved monitor was tested at KUR. The activities of ^{72}Ga in the monitors were measured just after their irradiations using an HP-Ge detector. The absolute fast neutron flux was deduced from the obtained activities with the improved sensitivity shown in Fig. 1. The results are summarized in Table 1. In the table, the nominal value means the value formally evaluated at KUR.

Table 1. Absolute fast neutron flux intensity obtained by the improved monitor.

	Experimental value (E)	Nominal value (C)	C/E
^{72}Ga activity*1 [Bq]	$(1.44\pm0.03)\times10^2$	—	—
^{72}Ga activity*2 [Bq]	$(1.48\pm0.04)\times10^2$	—	—
ϕ_{fast} [n/cm²/sec]	3.52×10^7	1.08×10^7	0.31

*1 For the PE type detector.
*2 For the B_4C type detector.
*3 The estimated error is about 38 %

From Table 1, the experimental value is larger than the nominal value by the C/E value of 0.31, while in the previous result the C/E value was 7.8. This means, the result was surely improved, however, it is still largely different from the nominal value. Consequently, though the monitor was modified, the monitor was confirmed not to be able to measure the fast neutron flux intensity properly. This is due to incoming scattered neutrons during irradiation, i.e., neutrons are scattered on the wall of the irradiation window and enter the detectors from outside of the collimator. Scattered neutrons cause an error of activity of the GaN foil and it leads to a large error between the experimental and nominal values. Now we are making further revisions of the design to shield scattered neutrons.

REFERENCES:
[1] K. Aoki, Master Thesis, Osaka Univ. (2021).
[2] S. Tada, Bachelor Thesis, Osaka Univ. (2022).

PR2-6 Neutron Image Sensor for Boron Neutron Capture Therapy

M. Taniguchi[1], T. Meguro[1], H. Tanaka[2], and S.-I. Kuroki[1]

[1]Research Institute for Nanodevice, Hiroshima University
[2] Institute for Integrated Radiation and Nuclear Science, Kyoto University Graduate School of Science, Kyoto University

INTRODUCTION: Boron neutron capture therapy (BNCT) has been attracting attention as an advanced treatment method on cancer, because of its merits with a minimally invasive and selective treatment. In the BNCT, for making therapy more accurate one, it is better to measure the neutron beam profile in real time. On the other hand, silicon carbide (SiC) semiconductor has a strong radiation hardness, and then is expected as base semiconductor for radiation hardened devices. The purpose of this study is to develop a two-dimensional neutron image sensor with SiC devices.

EXPERIMENTS: The structure of our neutron sensor is based on a three-transistor type image sensor pixel. The neutron sensor is based on an image sensor pixel using SiC, which has been developed in our laboratory, focusing on stable operation under neutron irradiation for a long time. The neutron sensors are equipped with boron-10 layer as a neutron conversion layer. In this layer, the injected neutrons have a reaction with boron-10, and then, alpha and lithium particles are emitted. The alpha particles penetrate the device, and generate electron-hole pairs, electrons are collected at gate electrode of SF(source-follower) transistor, and then the induced charge is detected as the output voltage from the sensor.

The neutron radiation experiments were carried out in KUR Heavy Water Neutron lrradiation Facility.

RESULTS: The neutron exposure experiment were carried out with neutron flux of $5x10^9$ $cm^{-2}s^{-1}$. The neutron sensor was biased with VDD=10 V, RST gate voltage of 0-10 V with pulse form. By the neutron beam exposure, the differential output voltage became 50 mV. The value was difference between output voltage with and without neutron beam. As the results, we can detect the neutron with this device. As the further study, we need to optimize the structure of the devices.

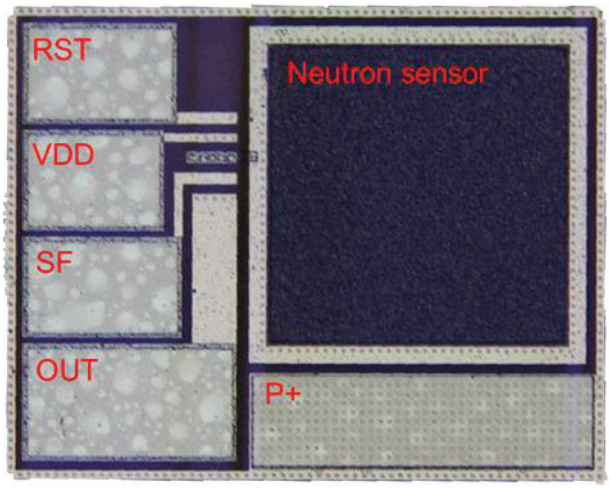

Fig. 1. SiC Neutron Sensor: This sensor consists of neutron sensor and three transistors.

REFERENCES:

[1] M. Tsutsumi *et al.,* IEEE Electron Device Lett., **44 (1)** (2023) 100-103.
[2] T. Meguro *et al.,* IEEE Electron Device Lett., **43 (10)** (2022) 1713-1716.

PR2-7 Preliminary survey of nuclide for epithermal neutron measurement using gel detector

Kenichi Tanaka, Yoshinori Sakurai[1], Tsuyoshi Kajimoto[2], Hiroki Tanaka[1], Takushi Takata[1], Satoru Endo[2]

Division of Liberal Arts Sciences, Kyoto Pharmaceutical University
[1]Institute for Integrated Radiation and Nuclear Science, Kyoto University
[2]Graduate School of Advanced Science and Engineering, Hiroshima University

INTRODUCTION: For boron neutron capture therapy, measurement of beam fluence spatial distribution is required for quality assurance in the irradiation field. This study investigated the use of the multi polymer gel detector system which consists of gels including different beam component converters. The preliminary selection of converter nuclide for epithermal neutrons is reported.

EXPERIMENTS: As an initial candidate, the $^{33}S(n,\alpha)^{30}Si$ reaction was considered based on the work of Porras [1] which showed a dose increase from the epithermal neutron component. As a method, the cross section library JENDL-4.0 was surveyed for the reactions with high cross section for epithermal neutrons [2]. Of particular interest were reactions that produced charged particles such as (n,p), (n,α), and (n,t) which result in charged particles depositing energy in the polymer gel detector. The data in Fig. 1 is an example of the cross section used in this study.

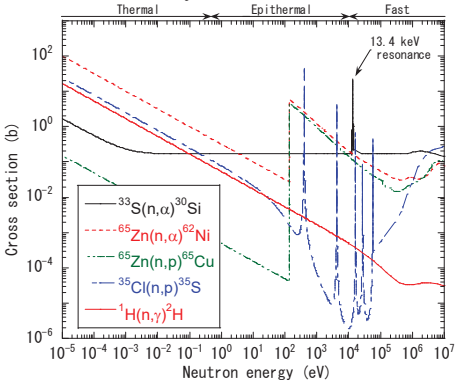

Fig. 1 Cross section used in this study.

RESULTS: The maximum of the cross section at each energy region of thermal (-0.5eV), epithermal (0.5eV-10keV), and fast (10keV-) is shown in Fig. 2, from the survey of nuclear reactions. The ratios of the cross section at the epithermal region in Fig. 2 to those at other regions are shown in Fig. 3. The reactions $^{65}Zn(n,\alpha)^{62}Ni$, $^{65}Zn(n,p)^{65}Cu$, and $^{35}Cl(n,p)^{35}S$ were selected as the candidates to enhance the epithermal neutron sensitivity of the gel detector. This is because their epithermal neutron cross sections in Fig. 2 and cross section ratios in Fig. 3 were comparable to those of $^{33}S(n,\alpha)^{30}Si$.

The nuclide ^{65}Zn with a half life of 244 days does not exist in nature, among the candidates selected. It should be produced by the neutron induction to ^{64}Zn (natural abundance: 49%). However, the reactions $^{65}Zn(n,\alpha)^{62}Ni$ and $^{65}Zn(n,p)^{65}Cu$ have a wide peak over 100 eV and low cross section at thermal and fast regions from Fig. 1, and they are expected to efficiently enhance the influence of epithermal neutrons than other candidate nuclides. Therefore, we decided to investigate ^{65}Zn as a promising option as well as ^{33}S and ^{35}Cl, apart from the convenience in practical use.

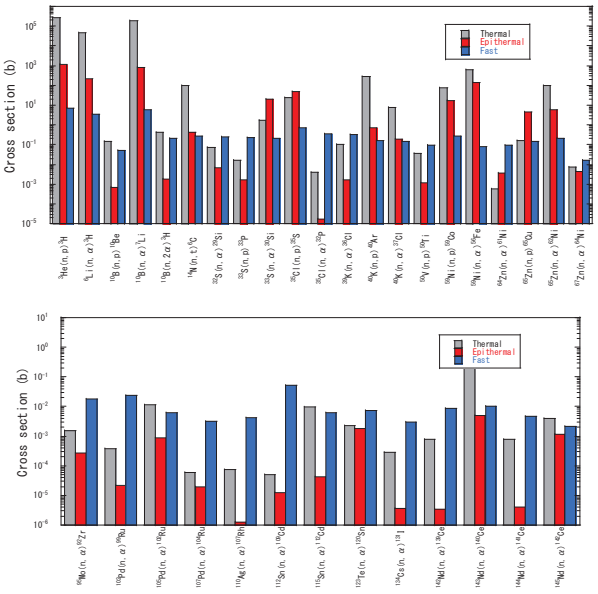

Fig. 2 Maximum cross section in energy range

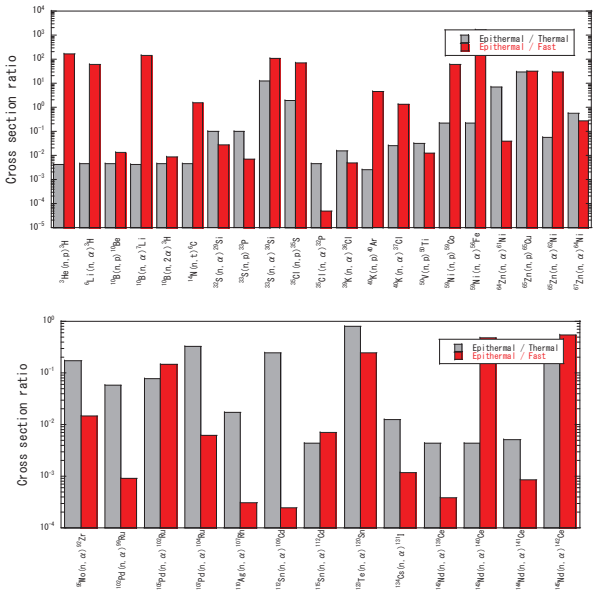

Fig. 3 Ratio of maximum cross section in epithermal region to that in other regions

REFERENCES:

[1] I.Porras *et al.* Appl. Rad. Isot. **69** (2011)1838-1841.
[2] K.Shibata *et al.* J. Nucl. Sci. Tech. 48 (2011)1-30.

Reviced: July 11th, 2023

PR2-8 Development and evaluation of 3D gel dosimeter for the measurement of dose distribution in BNCT

S. Hayashi, Y. Sakurai[1], M. Suzuki[1], and T. Takata[1]

Department of Clinical Radiology, Hiroshima International University
[1] Institute for Integrated Radiation and Nuclear Science, Kyoto University

INTRODUCTION: Three-dimensional (3D) gel dosimeters have been developed for the 3D dose measurement of complex dose distributions in clinical applications [1]. These devices utilize radiation-induced chemical reactions in the gel to preserve information about the radiation dose. The 3D absorbed dose distribution is deduced from the distribution of the reactant measured by imaging modalities, such as MRI (magnetic resonance imaging), X-ray CT (computed tomography), and optical CT. These gel dosimeters have excellent dose properties such as high sensitivity, dose rate independence, and a wide dose range, on X- and gamma-rays, and the potential as a 3D dosimeter has been expected.

In recent years, we have been studying the application of radiochromic gel dosimeters to dose evaluation in neutron irradiation. The optical dose-response of the PVA-I (PVA-GTA-I) radiochromic gel dosimeter [2, 3], which utilizes radiation-induced oxidation of iodide and its complex formation with polyvinyl alcohol (PVA), has been applied to neutron irradiation. The dose-response to beams with different energy spectra from a nuclear reactor has been studied and their availability has been investigated. Addition of a hydrated electron scavenger as a sensitizer showed significant dose-response improvement, while addition of boric acid as a neutron sensitizer significantly inhibited the fructose-induced initialization reaction.

Therefore, this year, we again optimized the composition, especially varying the concentration of fructose as a reducing agent and investigated its effect on the dose response.

EXPERIMENTS: The standard PVA-GTA-I gel dosimeter is composed of partially saponified PVA, potassium iodide (KI), glutaraldehyde (GTA), fructose, glucono-δ-lactone (GDL), and water, where fructose is a reducing agent and GDL is acid catalysis to promote the cross-linking, respectively. As sensitizers, boric acid $B(OH)_3$ containing ^{10}B of 20% naturally and potassium nitrate (KNO_3) as an electron scavenger were added into the gel dosimeter. A concentration of fructose was optimized to stabilize the dose-response property. The resulting solution was subdivided by pouring into PMMA cuvettes (4.5 mL, 1 cm path length). The neutron irradiations were performed using the Heavy Water Neutron Irradiation Facility (HWNIF) of Kyoto University Research Reactor (KUR, power of 1 MW). The samples were irradiated in the air at room temperature. The three different modes (thermal neutron-rich, epi-thermal and fast neutron-rich, and the mixed modes) of neutron beams made by heavy water spectrum shifter and cadmium thermal-neutron filters were applied to the samples.

RESULTS: Previously, it was feared that excess fructose would cause dosimeter fading. However, when we examined the dose-response at increasing fructose concentrations (0.1 M - 1.0 M), no significant fading was observed. In addition, the effect of suppressing autoxidation, which leads to an increase in the background, was also confirmed. It has been found that the rate of initialization can also be increased. On the other hand, excess fructose was also observed to inhibit responses at low doses. From the results of this work, it was found that the addition of about 0.3 M fructose is more effective. In the future, we plan to verify the effects of neutron sensitizer and other various sensitizers on the obtained new compositions.

REFERENCES:

[1] M. Marrale and F. d'Errico, Gels, **7** (2021) 74.
[2] S. Hayashi *et al.,* Radiat. Meas., **131** (2020) 106226.
[3] S. Hayashi *et al.,* J.Phys.; Conf. Ser., **2167** (2022) 012014.

PR2-9 Establishment of beam-quality estimation method in BNCT irradiation field using dual phantom technique (VI)

Y. Sakurai, N. Kondo, T. Takata, H. Tanaka and M. Suzuki

Institute for Integrated Radiation and Nuclear Science, Kyoto University

INTRODUCTION: Development in several types of accelerator-based irradiation systems for boron neutron capture therapy (BNCT) is underway. Many of these systems are nearing or have started clinical trials. Before the start of treatment with BNCT, the relative biological effectiveness (RBE) for the fast neutrons (over 10 keV) incident to the irradiation field must be estimated.
Measurements of RBE are typically performed by biological experiments with a phantom. Although the dose deposition due to secondary gamma rays is dominant, the relative contributions of thermal neutrons and fast neutrons are virtually equivalent under typical irradiation conditions in a water and/or acrylic phantom. Uniform contributions to the dose deposited from thermal and fast neutrons are based in part on relatively inaccurate dose information for fast neutrons.
The aim of this study is the establishment of accurate beam-quality estimation method mainly for fast neutrons by using two phantoms made of different materials, in which the dose components can be separated according to differences in the interaction cross-sections. The fundamental study of a "dual phantom technique" for measuring the fast neutron component of dose is reported [1].
In 2022, verification experiments for the dual phantom technique were performed using Heavy Water Neutron Irradiation Facility installed in Kyoto University Reactor (KUR-HWNIF) as in the previous year. Biological experiments were performed using the solid phantoms, which were made based on the simulation results [2].
MATERIALS AND METHODS: One of the dual solid phantoms was made of polyethylene with natural lithium fluoride for 30 weight percent (LiF-polyethylene phantom), and the other phantom was made of polyethylene with 95%-enriched lithium-6 fluoride for 30 weight percent (^{6}LiF-polyethylene phantom).
Glioblastoma U87MG ΔEGFR cells were cultured in Dulbecco Modified Eagle medium (DMEM) with 10 % fetal bovine serum in 5 % CO_2 incubator at 37 ℃. The cells were divided in two groups. One was p-boronophenylalanine (BPA, consisting of ^{10}B) treated group, and the other was non-treated group. The treatment group was cultured with 25 ppm BPA containing medium overnight.
The neutron flux and gamma-ray dose rate were measured using activation foils and thermo-luminescent dosimeter, respectively. The depth dose distributions for the thermal neutron, fast neutron and gamma-ray components were determined based on the simulation calculation results normalized referring to the measured values.
The epi-thermal neutron irradiation mode was used for the phantom experiments.
RESULTS: Figure 1 shows the cell survival fraction for the BPA administration group, BPA(+), and the non-administration group, BPA(-), in the LiF-polyethylene phantom. The items on the horizontal axis are arranged in ascending order of thermal neutron flux, such as "Control", "8-cm depth", "5-cm depth" and "2-cm depth". The values are normalized to be 1 with "Control" cells. "BPA(+)" corresponds to BPA-treated cell and "BPA(-)" corresponds to non-treated cell. The survival fraction became smaller as the thermal neutron flux became larger. The survival fraction for the non-treated cell was higher than that in BPA-treated cell.
Figure 2 shows the cell survival fraction in the ^{6}LiF-polyethylene phantom. The survival fraction showed no difference between non-treated and BPA-treated cells.
CONCLUSION: The ^{6}LiF-polyethylene phantom absorbs thermal neutrons although it has not significant effect in fast neutron dose. No difference in survival fractions between non-treated and BPA-treated cells with ^{6}LiF-polyethylene phantom indicated fast neutrons might not effect cell survival. On the other hand, due to mixture of thermal neutron in LiF-polyethylene phantom, BPA-treated cells were killed effectively compared with non-treated cells through n-alpha reactions.
ACKNOWLEDGMENT: This work was supported by JSPS KAKENHI Grant Number JP 16H05237.

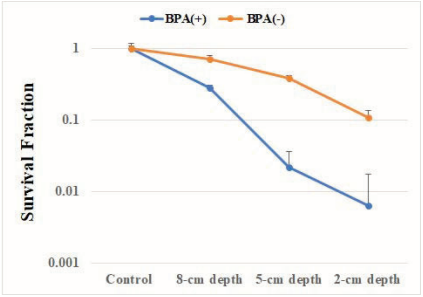

Fig. 1. Cell survival fraction in the LiF-polyethylene phantom.

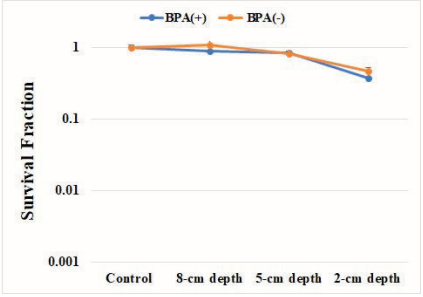

Fig. 2. Cell survival fraction in the ^{6}LiF-polyethylene phantom.

REFERENCES:
[1] Y. Sakurai *et al*., Med. Phys. **42** (2015) 6651-6657.
[2] Y. Sakurai and T. Kobayashi, Nucl. Instr. Meth. A, **453** (2000) 569-596.

PR2-10 Development of real-time boron-concentration estimation method using gamma-ray telescope system for BNCT

Y. Sakurai, D. Fu[1], T. Takata, H. Tanaka and M. Suzuki

Institute for Integrated Radiation and Nuclear Science, Kyoto University
[1]Graduate School of Engineering, Kyoto University

INTRODUCTION: It is important to decide the boron concentrations for tumor and normal parts in the dose estimation for BNCT. The on-line and real-time estimation method for the spatial distribution of boron concentration is expected for the advancement in dose estimation. The information about the boron concentration distribution can be obtained using the prompt gamma-ray analysis (PGA) for the 478-keV prompt gamma rays generated due to the nuclear reaction of boron-10 (B-10) with thermal neutrons.

The improved gamma-ray telescope system is settled at Heavy Water Neutron Irradiation Facility (HWNIF) of Kyoto University Reactor (KUR) [1-3]. This system is composed of an HPGe semiconductor detector and a collimation system including two lead collimators. The gamma rays through the two collimators can be detected, and the view-filed of the telescope can be expanded or reduced by moving the two collimators independently.

The experimental verification for the improved telescope system was performed. The experimental data was compared with the simulated data to calculate the specification coefficient.

MATERIALS AND METHODS: The phantom experiment was conducted in the irradiation room in KUR-HWNIF. The size of the phantom was 20 cm × 20 cm × 20cm. Within the phantom, a 5-cm diameter acrylic hollow sphere was placed as the tumor. Both the phantoms and tumor spheres were filled with different concentrations of boric acid water. The tumor spheres with the B-10 concentration of 70, 100, and 200 ppm were put into a phantom with B-10 concentration of 20 ppm.

The phantom was irradiated by the epithermal neutron irradiation mode. The irradiation field was set to 12 cm in diameter. Figure 1 shows the phantom and beam collimator placement in the irradiation room. The tumor sphere was fixed at the center of the telescope's view field. The 1st and 2nd telescope collimators were set at the bottom of the telescope (0-0 cm). A total of four irradiation experiments, including background tests, were conducted, each with an irradiation time of 15 minutes.

The specification coefficient is defined as $\tau = C/C`$, where C and C` are the experimental and simulated data, respectively. Regarding this coefficient, it is necessary to compare the counts of 478 keV prompt gamma rays in experiments and simulations with the same parameters. Since the input file of the detector in the simulation is made based on the energy distribution of the beam, and the data obtained from the simulation is flux, therefore the specification coefficients also carry the magnitudes. By comparing them with three B-10 concentrations of tumor spheres, the error in the calculation can be reduced.

RESULTS: From the experimental results, the spectra with different parameters were obtained. Figure 2 shows the spectrum from the experiment performed on a 70 ppm tumor sphere. The characteristic peaks are 478 keV for B-10 prompt gamma-ray, 511 keV for annihilation gamma-ray and 2220 keV for H-1 prompt gamma-ray. In the case of the 70 ppm tumor sphere, the experimental count rate was 29.6 cps (s^{-1}), simulated flux was 8.97×10^{-5} $cm^{-2}\cdot s^{-1}$, and the specification coefficient τ was 3.30×10^{5} $cps/cm^{-2}\cdot s^{-1}$. The average of the specification coefficient was calculated to 3.48×10^{5} $cps/cm^{-2}\cdot s^{-1}$, for the tumor spheres of 70 ppm, 100 ppm and 200 ppm.

CONCLUSION: From the results of the experimental verification, the effectiveness and usefulness of the improved gamma-ray telescope system were confirmed, and the specification coefficient was obtained. The more precise estimation will be performed for the B-10 concentration, size and position of the tumor sphere, and for the position of two telescope collimators. Moreover, the effective range for the discrimination between tumor and normal parts will be clarified.

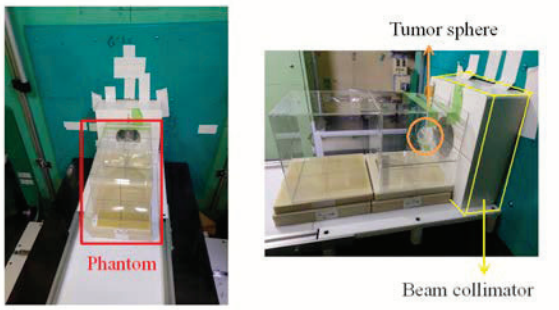

Fig. 1. Experimental setup for the phantom and beam collimator in the irradiation room of KUR-HWNIF.

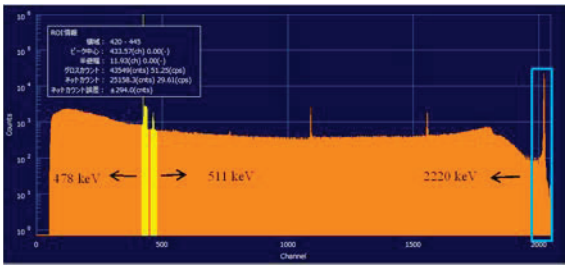

Fig. 2. The obtained spectrum from the experiment performed on a 70 ppm tumor sphere.

REFERENCES:

[1] Y. Sakurai *et al.,* Appl. Radiat. Isot., **61** (2004) 829-833.
[2] Y. Sakurai *et al.,* Appl. Radiat. Isot., **165** (2020) 109256.
[3] Y. Sakurai and T. Kobayashi, Nucl. Instr. Meth. A., **453** (2000) 569-596.

PR2-11 Development of scintillator for thermal neutron detector in BNCT

N. Matsubayashi, H. Tanaka[1], S. Kurosawa[2], A. Yamaji[2], T. Hanada[2], T. Takata[1]

Graduate School of Engineering, Kyoto University
[1] Institution for Integrated Radiation and Nuclear Science, Kyoto University
[2] Institution for Materials Research, Tohoku University

INTRODUCTION: Boron neutron capture therapy (BNCT) is a radiation therapy with thermal neutrons and ^{10}B. The particles emitted by the reaction of ^{10}B (n, α) ^{7}Li have cell dimensions and can selectively destroy tumor cells. In recent years, accelerator-based BNCTs have been constructed near hospitals, and clinical cases are increased. The activation method has been used for measurement of thermal neutron flux, but cannot measure in real-time. The development of neutron monitors capable in BNCT irradiation field is needed. The neutron monitor using Eu:$LiCaAlF_6$ (LiCAF) scintillator with quartz fiber was developed [1]. It is necessary for using the scintillator as neutron monitor to determine the relationship between the counts obtained by the detector and thermal neutron flux. Considering the increase in the clinical cases, we must calibrate the neutron monitor in primary national standard field. However, the neutron intensity of the standard field is much lower than that of the BNCT, and it takes about 5 days to calibrate the monitor available in BNCT. In this study, we develop new scintillator with faster response and higher detection efficiency than the LiCAF scintillator.

EXPERIMENTS: As the neutron detector in BNCT irradiation field, a scintillator with 0.3~0.6 mm long side is mounted on the tip of the fiber to reduce gamma-ray sensitivity. In this study, we selected the eutectic because very small scintillator can be used in BNCT irradiation field. LiBr/$CeBr_3$ and Ce:LiBr/$LaBr_3$ eutectic, which have fast response and high light yield, were grown and mounted on the fiber[2][3]. Since the grown scintillators are hygroscopic, they were packaged using glass and cement to prevent exposure to the outside air. The irradiation tests of each detector were performed in Cyclotron-based epithermal neutron source (C-BENS). The scintillator light entered the fiber and reached a photomultiplier tube (PMT). The signal from the PMT was then processed by a multi-channel analyzer (ANSeeN, ANS-HSMCA4416). To measure sensitivity to gamma-ray, the irradiation tests were carried out with ^{60}Co gamma-ray source.

RESULTS: Fig. 1 and 2 show the pulse height distributions of LiBr/$CeBr_3$ and Ce:LiBr/$LaBr_3$ in C-BENS and ^{60}Co gamma-ray source, respectively. As shown in Fig. 1 and 2, both scintillators have peaks corresponding to neutron event in the high channels. Comparing that of ^{60}Co gamma-ray source, it is confirmed that the eutectics can discriminate neutron and gamma-ray events. Since the neutron event obtained by LiCAF scintillator was observed near 720 Ch, we found that LiBr/$CeBr_3$ and Ce:LiBr/$LaBr_3$ have the same and twice the light yield of LiCAF, selectively. However, the neutron detection efficiencies of these eutectics were lower than that of LiCAF scintillator.

In conclusion, we developed neutron monitor for BNCT using LiBr/$CeBr_3$ and Ce:LiBr/$LaBr_3$ eutectic scintillator. The characteristics of these scintillators were not sufficient compared to conventional scintillator. However, the development of neutron monitors using a eutectic scintillator with hygroscopic has novelty. In the future, we will reselect the materials of scintillators and optimize the size and detection system.

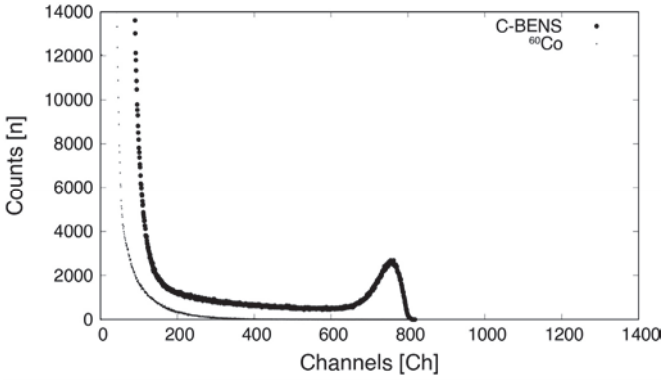

Fig. 1. Pulse height distribution of LiBr/$CeBr_3$ in C-BENS and ^{60}Co gamma-ray source.

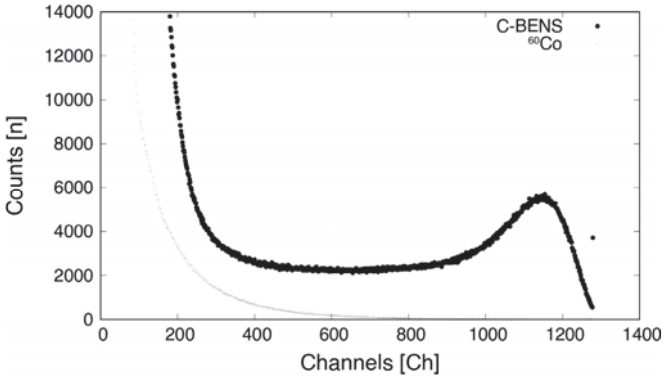

Fig. 2. Pulse height distribution of Ce:LiBr/$LaBr_3$ in C-BENS and ^{60}Co gamma-ray source.

REFERENCES:

[1] H. Tanaka *et al.*, Rev. Sci. Instrum., **88 (5)** (2017) 056101.
[2] R. Yajima *et al.*, Jpn. J. Appl. Phys., **61**, (2022) SC1028.
[3] Y. Takizawa *et al.*, Nucl. Instrum. Methods. Phys. Res A., **1028** (2022) 166384.

PR2-12 Quantitative Measurement of 478 keV Prompt Gamma-rays of Boron-neutron Capture Reaction

S. Komura, T. Mizumoto, Y. Sakurai[1], T. Takata[1], T. Tanimori[1], H. Kimura[2] and A. Takada[3]

J-BEAM Inc.

[1]*Institute for Integrated Radiation and Nuclear Science, Kyoto University*

[2]*Kyoto Pharmaceutical University*

[3]*Graduate School of Science, Kyoto University*

INTRODUCTION: In boron neutron capture therapy (BNCT), there is no method to measure the boron concentration in each tissue in the patient's body, which results in uncertainty in treatment planning. There is also no method to monitor the actual boron dose administered to the patient during neutron irradiation. Imaging of 478 keV prompt gamma rays produced by boron neutron capture reactions has the potential to solve these problems. To achieve quantitative imaging in neutron environments, we have been developing an electron tracking Compton camera (ETCC), which provides strong noise rejection by utilizing the information of the measured electron track. We conducted the following three types of experiments based on previous studies [1].

EXPERIMENTS AND RESULTS:

Exp. 1: We performed a three-dimensional prompt gamma-ray imaging test of a phantom using two ETCCs placed orthogonally to each other, as shown in Fig. 1. The phantom was a 45 mm tall tube with a 4.5 mm diameter, filled with a boric acid solution with a ^{10}B concentration of 1000 ppm. It was placed just above one of the ETCCs and irradiated with thermal neutron beam, with a diameter of approximately 1 cm, for 1.5 hours at E-3 under 1-MW operation. Both ETCCs successfully generated back-projection images of the phantom viewed from two different directions. The bright areas in both images corresponded well with the regions of the phantom that were irradiated by neutrons. Currently, we are conducting an integrated analysis of the data obtained from the two ETCCs to create a 3D image.

Exp. 2: A three-dimensional prompt gamma-ray imaging study of mice was performed in the same way as in Exp. 1. Nude mice, which were carrying U87MG tumors of approximately 1 cm in diameter on their shoulder, received a single dose of 1000 mg/kg BPA via tail vein injection. Each mouse was anesthetized, fixed in an acrylic container, and exposed to thermal neutron beams at the tumor site for 2 hours at E-3 under 5-MW operation. As in Exp. 1, we confirmed that the bright positions in the back-projection images of 478 keV gamma-rays corresponded well to the irradiation position of the mouse tumor . We are currently analyzing the data to create a 3D image.

Exp. 3: To demonstrate the effectiveness of ETCC in a real BNCT environment, we performed image monitoring of phantoms during neutron irradiation at HWNIF, as shown in Fig. 2. The phantom consisted of a 10-cm cubic acrylic container filled with a boric acid solution with a ^{10}B concentration of 230 ppm. The 478 keV prompt gamma rays emitted from the phantom passed through a cylindrical hole in the ceiling and were measured by ETCC. In a previous experiment conducted last year, the phantom was successfully imaged during 1-MW operation. This year, we switched the gas used in the gaseous electron tracker of ETCC from Ar-based gas to Ne-CF4 mixed gas to reduce accidental coincidence noise at high counting rates. At 1-MW operation, we obtained a gamma-ray image with a better signal-to-noise ratio than with conventional gases. However, under 5-MW operation, although ETCC operated stably, the gamma-ray image did not correspond well with the phantom installation position. We are currently analyzing the causes.

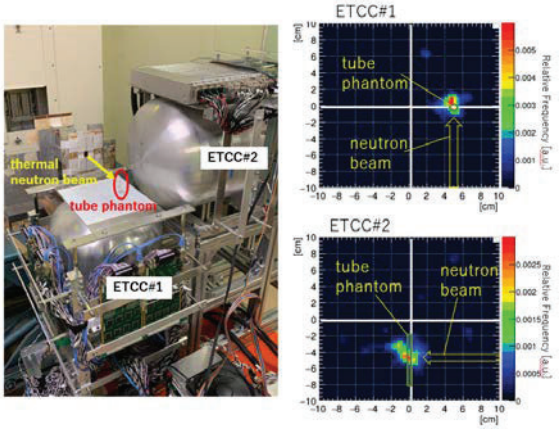

Fig.1. Photograph and measured 478 keV gamma-ray images in Exp.1.

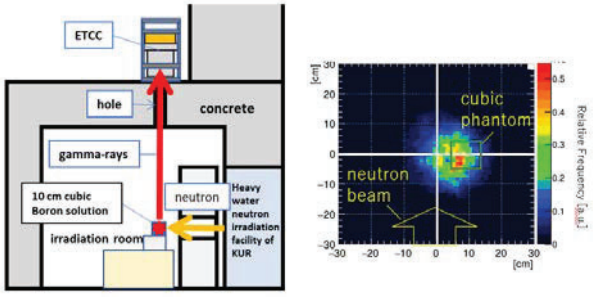

Fig.2. Schematic view and measured 478 keV gam-ma-ray image at 1-MW operation in Exp.3.

REFERENCES:

[1] T. Mizumoto *et al.*, KURNS Progress Report 2021.

PR2-13 Visualization of Boron Dose Distibution on a Borosilicate Glass Plate by Neutron Irradiaiton

A. Nohtomi, Y. Kojima, H. Maeda, T. Yamane, G. Wakabayashi[1], Y. Sakurai[2] and T. Takata[2]

Graduate School of Medicine, Kyushu University
[1]Atomic Energy Research Institute, Kindai University
[2]Institute for Integrated Radiation and Nuclear Science, Kyoto University

INTRODUCTION: Boron dose plays a critical role to kill tumor cells for the boron-neutron capture therapy (BNCT). Therefore, simple method of boron dose distribution measurement is much desirable for QA/QC purposes of BNCT. In the present study, boron dose distribution on a borosilicate glass plate, in which contains approximately 4 wt% natural boron (Table 1), has been visualized by using a CMOS camera during thermal neutron irradiation. High energy lithium ion and alpha particles generated by ^{10}B-neutron capture reactions were detected by the glass itself which acted as scintillator.

EXPERIMENTS: A borosilicate glass plate (100 x 100 x 20 mm^3, COSMOS VID Co., LTD.) was irradiated by thermal neutrons (~10^6 n/cm^2/s) during 600 s and 1200 s at E-3 irradiation port of KUR [1]. Luminescence of the glass plate was observed by a cooled CMOS camera (BITRAN, CS-67M) during the irradiation in a black box as shown in Fig. 1. For comparison, another soda lime glass plate (100 x 100 x 19 mm^3, COSMOS VID Co., LTD.) was irradiated and observed in the same manner.

RESULTS: As shown in Fig. 2, when the borosilicate glass plate was irradiated by neutrons, the cross section of beam profile was clearly visualized as luminescence distribution for 1200 s neutron irradiation. When the irradiation time was 600 s, the luminescence was weaker than that for 1200 s. On the other hand, no visible luminescence was observed for the soda lime glass, in which boron was not contained. The beam profile obtained by the borosilicate glass plate was compared with that measured by the decaying self-activation method of a CsI scintillator plate at the exit window of E3-port [2]. As indicated in Fig. 3, both profiles evaluated by different methods showed a reasonable agreement.

From the facts described above, it is evident that the observed luminescence is originated from lithium ion and alpha particles generated by ^{10}B-neutron capture reactions. This technique will be applicable for the daily QA/QC purposes of BNCT, because instantaneous neutron irradiation may be enough for observation of the actual intense neutron beam of clinical BNCT field (~10^9 n/cm^2/s).

Table 1. Typical composition and density of general glass.

	Composition (wt%)						Density (g/cm^3)
	SiO_2	B_2O_3	Al_2O_3	Na_2O/K_2O	CaO	others	
borosilicate glass	81	13	2	4	-	-	2.2
soda lime glass	70～74	-	0～2	12～16	6～12	MgO	2.5
quartz glass	100	-	-	-	-	-	2.2

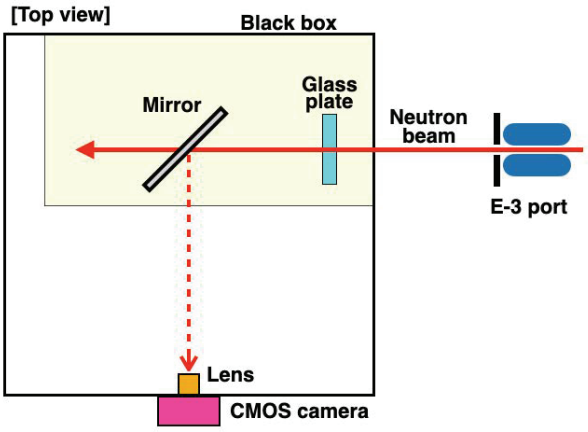

Fig. 1. Schematic drawing of experimental arrangement.

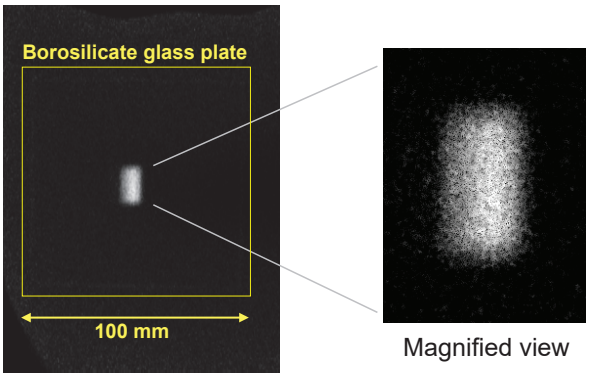

Fig. 2. Visualized boron dose distribution on a borosilicate glass plate observed by a CMOS camera during 1200 s neutron irradiation.

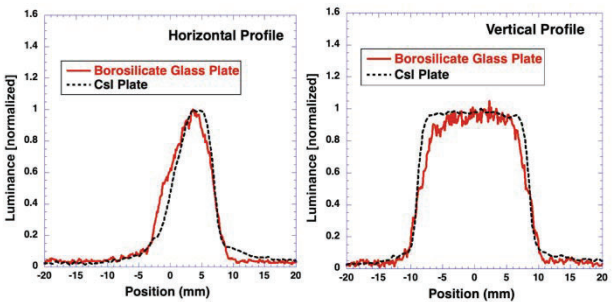

Fig. 3. Comparison between the profile obtained by luminescence of borosilicate glass plate and that measured by the self-activation of a CsI plate.

ACKNOWLEDGEMENT: This work was supported by JSPS KAKENHI Grant Number JP19K08202 and JP22K07697.

REFERENCES:

[1] T. Kobayashi and, K. Kand, Nucl. Instrum. Meth., **204** (1983) 525-531.
[2] A. Nohtomi *et al.*, Radiol. Phys. Technol., **15** (2022) 37-44.

PR2-14 Investigation of Thermal Neutron-Induced Soft Errors in Semiconductor Devices

H. Tanaka, R. Nakamura[1], and T. Kato[1]

Institute for Integrated Radiation and Nuclear Science, Kyoto University
[1]Reliability and Engineering Department, Socionext Inc.

INTRODUCTION: Soft errors are radiation-induced errors in semiconductor devices. With aggressive scaling down of transistor size and operating voltage, the semiconductor devices are becoming more susceptible to the soft errors. Therefore, to assess the reliability of electronic systems, it is necessary to investigate the characteristics of the soft errors.

In the terrestrial environment, the major radiation source for the soft errors is cosmic-ray-induced neutrons. The energy spectrum of the terrestrial neutron ranges from thermal to high-energy. The semiconductor devices are sensitive to the thermal neutrons when the devices contain abundant ^{10}B atoms, which produces He and Li ions through neutron-induced fission reactions [1].

It has been reported that in recent semiconductor devices the thermal neutron-induced soft errors appear due to the contamination of ^{10}B atoms during manufacturing processes [2, 3]. In previous experiments, the authors have demonstrated that the detailed characteristics of the thermal neutron-induced soft errors in static random-access memories (SRAMs) [4].

This study investigates the thermal neutron-induced soft errors in an advanced SRAM. Soft error rates (SERs), which are the occurrence rates of radiation-induced errors, are evaluated by neutron irradiation testing at KUR.

EXPERIMENTS: Neutron irradiation tests were performed using Heavy Water Neutron Irradiation Facility (HWNIF) of KUR [5]. The irradiation modes used were "OO–0000F" and "CO–0000F." Fig. 1 shows the energy spectra of these modes together with that of the terrestrial environment [6]. The "OO–0000F" and terrestrial spectra are similar to each other. This means that the neutron source is suitable for the investigation of the terrestrial neutron-induced soft errors. The thermal neutron sensitivity was examined by comparing results between the "OO–0000F" and "CO–0000F" modes.

The test samples were SRAM chips manufactured in an advanced CMOS process, which were labeled as Device C. During the irradiation, the SRAM chips were remotely operated, and the error events were measured. The SERs were then statistically calculated according to the JEDEC standard [7]. Thermal neutron fluxes at the locations of the samples were measured by the gold activation method. The results were compared with the previous results for Device A and B.

RESULTS: Fig. 2 presents the measured SERs of Device A, B and C, where the results of "OO–0000F" and "CO–0000F" are shown. Note that the SER values are normalized by the value of Device A with "OO–0000F".

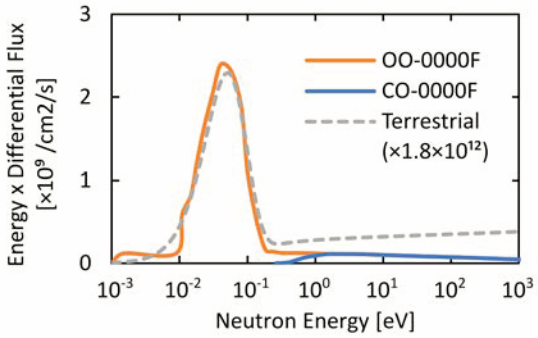

Fig. 1. Neutron energy spectra of KUR HWNIF [5] and terrestrial environment [6] .

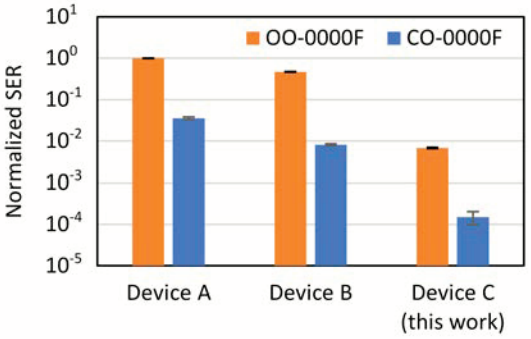

Fig. 2. Measured SERs of Device A, B and C for "OO–0000F" and "CO–0000F" modes.

For Device C, the SER of "CO–0000F" was significantly lower than that of "OO–0000F," as similarly observed in Device A and B. This result clearly shows that Device C is sensitive to thermal neutrons and contains nonnegligible amounts of ^{10}B atoms.

At the same time, the SER for Device C was greatly reduced compared to Device A and B. This indicates that the concentration of ^{10}B atoms for Device C is lower than Device A and B because basically the thermal neutron SER is proportional to the ^{10}B concentration.

Our experiments successfully demonstrated the difference in the thermal neutron sensitivity of the three SRAM devices. This result suggests that thermal neutron irradiation testing is essential to assess the soft error reliability.

REFERENCES:

[1] R. Baumann *et al.,* Proc. IEEE Int. Reliab. Phys. Symp. (IRPS), **152** (2000).
[2] S. Wen *et al.,* Proc. IEEE Int. Reliab. Phys. Symp. (IRPS), **SE.5.2** (2010).
[3] Y. Fang *et al.,* IEEE Trans. Device Mater. Rel., **14** (2014) 583.
[4] T. Kato *et al.,* IEEE Trans. Nucl. Sci., **68** (2021) 1436.
[5] Y. Sakurai *et al.,* Nucl. Instr. Meth. A, **453** (2000) 569.
[6] T. Sato, PLoS ONE, **10(12)** (2015).
[7] JEDEC Standard JESD89A (2006).

PR2-15 Dosimetric Characteristics of Optimized Bolus for Boron Neutron Capture Therapy

T. Takata, M. Nojiri[1], A. Sasaki[1], Y. Sakurai, H. Tanaka and M. Suzuki

Institute for Integrated Radiation and Nuclear Science, Kyoto University
[1]Graduate School of Engineering, Kyoto University

INTRODUCTION: In Boron Neutron Capture Therapy (BNCT), an epithermal neutron beam has been utilized to penetrate a deep site of a patient's body. However, thermal neutron buildup near a beam incident surface, associated with thermalization of epithermal neutrons, causes dose deficiency in a case where a tumor extends to vicinity of patient surface. For such a case, a thermal neutron compensation bolus consisting of a hydrogen-rich material has been utilized to improve the dose distribution. In present clinical BNCT, a bolus with a uniform thickness and a simple shape has been adopted. This study aims to increase the dose ratio of tumor to normal tissues more aggressively, by optimizing the bolus shape. An overview of the optimizing method was described in the previous report [1]. Verification using a water phantom has been attempted through experimental measurements, where the phantom with/without a simple-shaped bolus were used [2,3]. In this report, we describe comparison of dosimetric characteristics between the cases without bolus, with rectangular bolus and the optimized bolus.

MATERIALS AND METHODS: A cylindrical water phantom with a height of 20 cm and diameter of 20 cm was used, assuming a head-and-neck case with a parotid gland cancer irradiated from the lateral direction. A spherical volume with a 4-cm diameter centered at a 2-cm depth from the side surface of the cylinder was defined as a planning target volume (PTV), assuming a tumor extended to a subcutaneous region. A tubular volume with a 3-cm diameter along the center axis of the cylinder was defined as an organ at risk (OAR), assuming a mucosal tissue of oral cavity and pharynx [2].

Dose calculations were performed by using SERA, a treatment planning system for BNCT, for the cases without bolus, with rectangular bolus and the optimized bolus [4]. Figure 1 shows the geometry modeling in SERA for these cases. The rectangular bolus with the dimension of 7.5 × 7.5 × 1.1 cm^3 and the optimized bolus, each modeled as light-water region, were mounted on the beam axis on the side surface of cylinder. The optimization procedure of bolus shape was described in detail in Ref.1 and 2. An epithermal neutron beam of KUR Heavy Water Neutron Irradiation Facility with an aperture of 12-cm diameter was assumed in the calculations [5].

RESULTS AND DISCUSSION: Figure 2 shows the depth distributions of thermal neutron flux along the beam axis calculated for three cases. The figure also shows the measured distributions with adjusted depth for the cases without bolus and with the rectangular bolus [3]. In the case without bolus, thermal neutron buildup caused reduction of flux in the shallower region, resulting in lower minimum dose of PTV. In the case with the rectangular bolus, the distribution shifted toward the depth direction and the dose in the shallow region was increased. In the case with the optimized bolus, the PTV region had equalized fluxes at the entrance and distal sides, leading to higher dose coverage. However, minimum dose of the PTV was comparable between for the cases with rectangular and optimized bolus under constraint of OAR dose. The optimization method needs to be improved to further increase PTV dose.

ACKNOWLEDGMENT: This work was supported by JSPS KAKENHI Grant Number JP 17K17838.

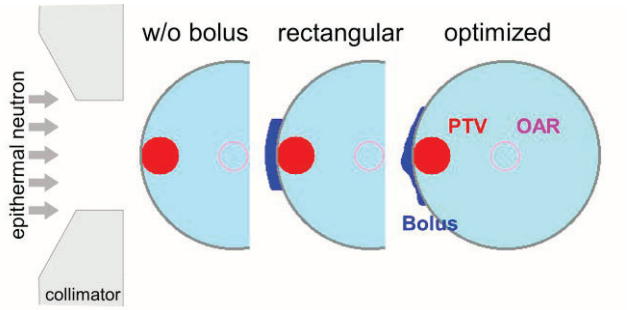

Fig. 1. Modelling of cylindrical water phantom without bolus, with rectangular bolus and with optimized bolus.

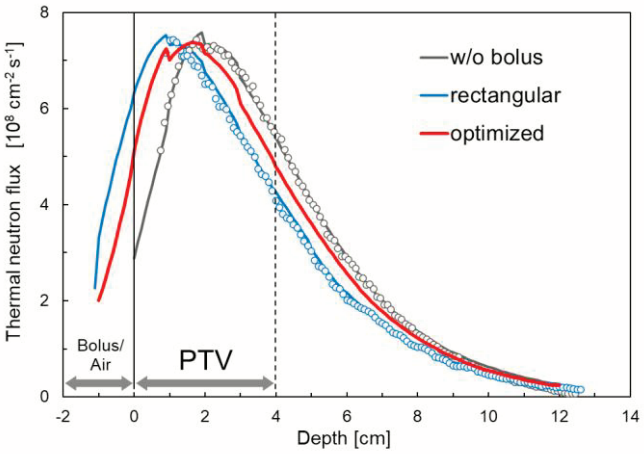

Fig. 2. Depth distributions of thermal neutron flux for cases without bolus, with rectangular bolus and with optimized bolus.

REFERENCES:

[1] T. Takata *et al.*, KURNS Progress Report 2019, (2020) 56.
[2] T. Takata *et al.*, KURNS Progress Report 2020, (2021) 83.
[3] T. Takata *et al.*, KURNS Progress Report 2021, (2022) 68.
[4] D. E. Wessol *et al.*, INEEL/EXT-02-00698 (2002).
[5] Y. Sakurai and T. Kobayashi, Med. Phys., **29** (2002) 2328-2337.

PR2-16 Three dimentional humanized oral cancer in vitro model for BNCT

K. Igawa, K. Izumi[1], E. Naito[1], M. Suzuki[2], N. Kondo[2], Y.Sakurai[2]

Neutron Therapy Research Center, Okayama University

[1] Graduate School of Medical and Dental Sciences Oral Life, Niigata University

[2] Institute for Integrated Radiation and Nuclear Science, Kyoto University

INTRODUCTION:
The preclinical animal test for BNCT is challenging from the ethical point of view of animal welfare and animal protection, as well as from the legal point of view of animal management in radiation-controlled areas. Since only a few facilities in Japan are capable of performing neutron irradiation tests on animals, there is a strong demand for alternative animal test models.
Recently, the various three-dimensional (3D) cancer models such as spheroids, organoids, and scaffold-based constructs have been developed and widely used in cancer research due to their ability to mimic multiple features of the tumor microenvironment. The 3D models are promising for the safety and efficacy assessment. Therefore, we have developed the 3D oral cancer in vitro model with human oral cancer cells and patient derived normal oral fibroblasts for BNCT. The optimal conditions of the 3D oral cancer model for BNCT have been inves-tigated. In this study, we report the histopathological fea-tures of 3D oral cancer model after BNCT.

EXPERIMENTS: First, we fabricated humanized 3D oral cancer in vitro model. The patient derived oral mucosal fibroblast cells（Niigata University, 2015-5018 ） were embedded and cultured on type I -A collagen (Nii-tagelatin, Japan) for 7 days and oral squamous cell lines （HSC3, Riken Cell Bank）were seeded on the top of surface of 3D collagen matrix for additional 7days in α MEM medium (Wako, Japan) supplemented with 10 % fetal bovine serum (Sigma -Aldrich, USA) and 100 unit/ml penicillin and 100 μg/ml streptomycin (1% p/s) (Thermo Fisher Scientific, USA) [1]. Next, before neu-tron irradiation, Boron (Steboronine®, Stella pharma, Japan) or Phosphate Buffered Saline （PBS, Sigma -Aldrich, USA）was added to the oral 3D model and incubated for 2 hours and washed by PBS. The 3 D mod-els were irradiated by neutron for 20 minutes and cul-tured under a humidified atmosphere of 5% CO_2 at 37 ◦C for 2 hours for another 3 days. Finally, the 3D models were fixed with 10 % formalin, embedded in paraffin, cut in 5 μm sections and stained with hematoxylin and eosin. All images of the sections were obtained with an all-in-one fluorescence microscope (BZ-X800, KEYENCE, Osaka, Japan). The data are shown as means± standard deviation (S.D.) A p-value of less than 0.05 was considered statistically significant.

RESULTS: The histological examinations of the 3D oral cancer model after 3days of neutron irradiation were shown in Figure 1 and Table 1. The thickness of the HSC cells layer in the model after BNCT reduced from the multilayer to monolayer. However, there are no difference in the thickness of fibroblast-embedded collagen gel between the two (Figure 1). The size of HSC cells in the 3D oral cancer model after BNCT became about twice as large compared to the control, on the other hand, the fibroblasts was the same size with or without BNCT (Table 1) . These results indicate the 3D humanized oral cancer in vitro model would be an alternative tool to animal test for BNCT.

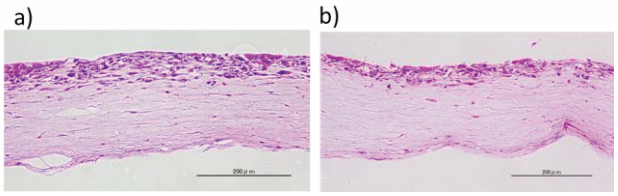

Figure 1. Microscopic image of the histological section of 3D oral cancer in vitro model at 7 days after neutron irradiation. (a) Control, (b)BNCT.

Table 1. BNCT induced histological changes 3D oral cancer in vitro model.

	Control	BNCT
Cancer cells layer [layer]	7.0±1.8	2.5±1.3
Tumor area rate [%]	21.6 ±2.7	16.7±1.4
Size of a cancer cell [μm²]	51.6±8.9	125.6±57
Stromal tissues area rate [%]	78.4±4.6	83.3±3.7
Size of a fibroblast [μm²]	48.5±29	43.9±12

DISCLOSURE: This research was partially supported by JSPS KAKENHI Grant Number JP20K12714.

REFERENCES:
[1] K. Haga *et al.,* Translational Oncology **12** (2021) 101236.
(doi)10.1016/j.tranon.2021.101236

PR2-17 Boron-10 uptake distribution in 3D oral cancer model using CR-39 solid state nuclear track detector

K. Igawa, R. Ogawara[1], T. Kusumoto[2], and Y. Sakurai[3]

Neutron Therapy Research Center, Okayama University

[1] Advanced Research Center for Beam Science, Institute for Chemical Research, Kyoto University

[2] Center for Advanced Radiation Emergency Medicine, National Institutes for Quantum and Radiological Science and Technology

[3]Institute for Integrated Radiation and Nuclear Science, Kyoto University

INTRODUCTION:

Boron neutron capture therapy (BNCT) for oral cancer is expected as a function-preserving therapy to maintain and improve the quality of life of cancer patients. The key to the success of BNCT is to accurately confirm the distribution of boron accumulation in the tumor and surrounding the normal regions including the tumor margins. Then, we have developed an estimation system for absolute values of a boron-10 uptake distribution in a tissue slice measured by single tracks from 10 B(n, α) 7 Li reactions using CR-39 nuclear track detector at accelerator-based neutron field.

Recently, the various three-dimensional (3D) cancer models such as spheroids, organoids, and scaffold-based constructs have been developed rapidly and are promising for the safety and efficacy assessment compared with simple 2D model. The patient delivered 3D model has demonstrated high predictive performance to predict the clinical response of the new cancer treatment. We have also developed the 3D oral cancer in vitro model with human oral cancer cells and patient derived normal oral fibroblasts for the radiation treatment.

In this study, using CR-39 nuclear track detector, the boron distribution and concentration of oral cancer regions in 3D oral cancer in vitro models is validated.

EXPERIMENTS:

The 3 D oral cancer in vitro model was fabricated with human primary normal oral fibro-blasts（Niigata University 2015-5018）and the human oral squamous carcinoma cell lines（JCRB）. The 3D oral cancer model administered with Boron (Borofaran, Stella pharma, Japan) for 2 hours was cleaned by PBS twice and embedded by O.C.T. compounds (Tissue Tek, Sakura, Japan) on a dry ice. The section at a range of 5 μm was mounted on the CR-39 plastic nuclear track detector (TechnoTrack, Chiyoda Technol Corp., Japan) using cryostat. After the neutron irradiation (KURRI) of 3D oral cancer tissue on the surface of CR-39, the tissue was removed from the CR-39. After chemical etching by a potassium hydroxide-ethanol-water (PEW-45; KOH 15 wt%, ethanol 45 wt%, water 40wt%), the microscopic image of a-particle tracks on the CR-39 was acquired with a high-speed imaging microscope (HSP-1000, SEIKO Time Systems Inc., Tokyo, Japan).

RESULTS:

The histological section of 3D oral cancer model on surface of CR-39 was irradiated for 20 mins at 2 X10^{12}/cm^2 thermal neutron fluence. The growth of etch pit diameter of a CR-39 was 3.5 μm controlled by PEW-45 at 50 ℃. The microscopic images of etch pits on CR-39 detectors were obtained as shown Figure 1 A. The number of etch pits in tumor regions (Figure 1 A-❶)was significantly higher than in stromal regions（Figure 1 A-❸）. After the analysis of etch pits, the etch pit density distribution map of a histological section 3D oral cancer model was acquired as shown Figure1 B. The results indicated that the boron concentration in tumor regions was significantly higher than in stromal regions. However, the quantitative analysis was difficult in high boron concentration areas. The further studies are needed for the optimal etch pits analysis for the 3D oral cancer model.

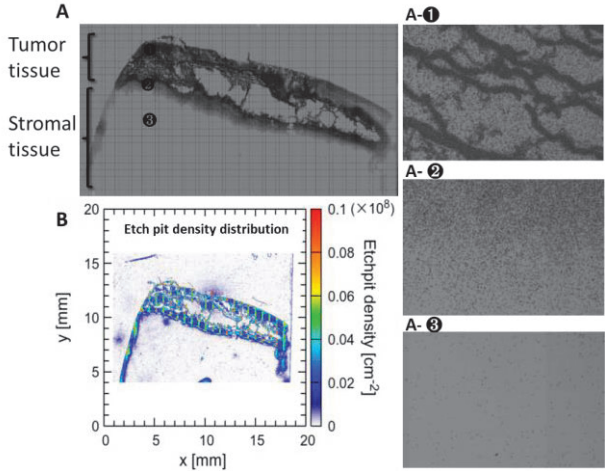

Figure 1. A）Microscopic images of a histological section of 3D oral cancer model and etch pits of CR-39 after neutron irradiation. The microscopic images of etch pits of CR-39 at ❶tumor regions ❷tumor margins ❸stromal regions. B）Etch pit density distribution map of a histological section of 3D oral cancer model.

DISCLOSURE: This research was partially supported by JSPS KAKENHI Grant Number JP20K12714.

REFERENCES:

[1] K. Haga *et al.,* Transl Oncol., **14(12)** (2021) 101236.

[2] T. KONISHI *et al.,* J. Radiat. Res., **48** (2007) 225-261.